Energy Conversion and Management 198 (2019) 111852

Contents lists available at ScienceDirect

Energy Conversion and Management

journal homepage: www.elsevier.com/locate/enconman

Reduction of efficiency penalty for a natural gas combined cycle power plant with post-combustion CO_2 capture: Integration of liquid natural gas cold energy

Junjiang Bao, Lei Zhang, Chunxiao Song, Ning Zhang, Minggang Guo, Xiaopeng Zhang*

State Key Laboratory of Fine Chemicals, School of Petroleum and Chemical Engineering, Dalian University of Technology, Panjin 124221, China

ARTICLE INFO

Keywords:
LNG cold energy
Heat exchange network
Thermal integration
CO_2 capture
NGCC

ABSTRACT

The high energy consumption requirements of the post-combustion CO_2 capture (PCC) process of a natural gas combined cycle (NGCC) power plant will result in a significant reduction in power generation efficiency, and the energy integration of the system can effectively reduce power plant efficiency penalties. However, the existence of a large amount of low-temperature waste heat in NGCC power plant is difficult to utilize due to its low temperature. In this paper, the integration of LNG cold energy with NGCC power plant with PCC process is proposed. For the 391 MW NGCC plant with MEA-based PCC system, the impact of the exhaust gas recirculation (EGR) process is firstly considered and a basic case of 35% EGR is obtained. Then the internal energy integration of the NGCC + PCC + EGR system (case 1) reveals that there are a large number of different temperature waste heat sources in the system, and then the dual-pressure ORC is integrated into the system for energy integration (case 2). Finally, in order to integrate the low temperature waste heat that has not yet been utilized and recover the cold energy of LNG, the LNG and the two-stage condensation Rankine cycle are integrated with case 2. The results show that the net power output of case 3 is 17.55 MW higher than that of NGCC + PCC + EGR system, the total efficiency is increased by 2.51%, and the efficiency penalty is reduced to 7.9%. It can be seen that the combination of LNG cold energy and NGCC power plant can effectively improve the power generation efficiency and reduce the energy penalty.

1. Introduction

In recent years, the rapid development of the economy has steadily increased demand for electricity, while low cost, high calorific value of fossil fuels, such as coal and natural gas, are widely used in power plants [1]. The problem is that greenhouse gas emissions lead to global warming, sea level rise and so on. To slow down the rise of global average temperatures, countries around the world signed the *Paris agreement* in 2015 calling for lower CO_2 emissions. On the other hand, solar energy [2], wind energy [3], geothermal energy [4] and other clean energy sources have been developed rapidly. Even so, fossil energy will remain the main source of energy in the near future. Among them, the power generation capacity of NGCC power plants currently accounts for more than 20% of global power generation, the net power generation efficiency of NGCC power plants can reach 55%-60% [5–7], and the CO_2 generated by unit power generation is only half of that of coal-fired power plants [1]. In order to achieve the target of CO_2 emission reduction, the proportion of NGCC power plants with CO_2 capture compression technology will increase gradually.

There are three kinds of CCS technology used in power plants, namely pre-combustion capture [8], post-combustion capture [9,10], and O_2-fuel combustion capture [11,12]. Among them, post-combustion capture has been widely concerned because it can be directly modified and the method is mature. There are many options for CO_2 post-combustion captures technology, such as MEA-based chemical solvent processes [13], adsorption processes [14–16], multi-stage membrane processes [17,18] and temperature swing adsorption processes [19,20]. The absorption process of monoethanolamine (MEA) solvent which has been widely used post-combustion due to its good absorption effect, large treatment capacity and its mature technology. And it can also be operated at atmospheric pressure and low CO_2 concentration. A summary of the literatures on NGCC power plant and MEA-based CO_2 capture progress are given in Table 1.

From Table 1, it could be found that the PCC process of the NGCC power plant will result in high efficiency penalty, and the overall power generation efficiency is decreased by about 6–10% [37], where the unit

* Corresponding author.
E-mail address: xiaopengzhang@dlut.edu.cn (X. Zhang).

https://doi.org/10.1016/j.enconman.2019.111852
Received 13 June 2019; Received in revised form 16 July 2019; Accepted 17 July 2019
Available online 20 July 2019

Nomenclature

Acronyms

NGCC	natural gas combined cycle
LNG	liquid natural gas
PCC	post-combustion CO_2 capture
EGR	exhaust gas recirculation
ORC	organic Rankine cycle
TSCRC	two-stage condensation Rankine cycle
CCR	CO_2 capture rate
TI	thermal integration
PC	power consumption
HP	high pressure
HPP	high pressure pump
IP	intermediate pressure
IPP	intermediate pressure pump
LP	low pressure
LPP	low pressure pump
RP	recirculation pump
GT	gas turbine
ST	steam turbine
ECON	economizer
HRSG	heat recovery steam generator
RHT	reheater
SPHT	superheater
DESHT	desuperheater
Sep	separator
DP	dual pressure

Symbols

n	molar flow rate [kmole·s^{-1}]
m	mass flow rate [kg·s^{-1}]
p	pressure [bar]
LHV	Lower heating value
Q	heat [MW]
W	work [MW]
s	specific entropy [kJ·kg^{-1}·K^{-1}]
T	temperature [K]
η	efficiency

Subscripts

aux	Auxiliary power
net	net power output
mech	mechanical
gen	generator
reb	reboiler
comp	compressor
turb	turbine
in	inlet
out	outlet
i	different configurations of NGCC power plants

energy consumption of CO_2 capture is usually 2.8–5.8 GJ/ton CO_2. This unit energy consumption of CO_2 capture is much larger than 2.6 GJ/ton CO_2 with CO_2 concentration of 11%, which is a value of ideal operating status according to the novel and effective thermodynamic cycle proposed by Wang et al. [34]. Due to the huge global power consumption and the high efficiency penalty of PCC process in power plants, the development of carbon capture technology will be limited to a certain extent. The reduction of energy consumption in PCC process can be realized by changing the system structure. For example, by the exhaust gas recirculation process, it is found that the concentration of CO_2 in flue gas is increased, the energy consumption of CO_2 captured system is reduced, and the net power generation efficiency of power plant is improved. The power plants assisted by solar or biomass can also reduce system energy penalty. For example, T. Lambert et al. [26] used solar energy to assist the CO_2 capture of NGCC power plant with EGR process. Thermodynamic analysis Another way is utilizing the waste heat of power plants to improve the power output of the NGCC system. For example, G.G. Esquivel-Patiño et al. [5] studied the potential of thermal integration of power plants and the power generation of ORC, and the efficiency of power plants increased from 50.69% to 50.94%.

According to the literature review above, the power generation efficiency of the NGCC system can be improved by changing the structure of the power plant and using ORC to recover the waste heat. However, it can also be found that in the integration process, a large amount of low temperature waste heat in the power plant cannot be utilized by the ORC using cooling water as a heat sink. Therefore, in this paper, the idea of using LNG cold energy and NGCC power plant with PCC process is proposed. First of all, the NGCC power plant with PCC process are constructed and validated, and then the improvement rate of the EGR process on power generation efficiency is investigated. On this basis, the power generation efficiency of the system is improved by using thermal integration and ORC to recover a large number of waste heat from different temperature levels in the power plant. Finally, LNG cold energy is integrated with NGCC system in order to further improve the efficiency of power generation.

2. System descriptions

Fig. 1 shows the schematic diagram of a NGCC power plant with PCC and EGR processes. The NGCC power plant is composed of a gas turbine and steam turbines, and the PCC process consists of two parts: CO_2 capture unit by MEA-based absorption process and CO_2 compression and liquefaction process. The PCC process needs steam extraction from steam turbine to supply reboiler.

The power auxiliary part includes the energy consumption of the CO_2 compression process, water circulating pumps, cooling pumps and amine circulating pumps of the NGCC power plant, which is provided by NGCC power plant. The specific flow chart and principle of each system can be found in Sections 2.1–2.2.

2.1. NGCC power plant process

The schematic diagram of the NGCC power plant is shown in Fig. 2. Its main equipment includes: air compressor (AC), combustion chamber (Comb), gas turbine (GT) and heat recovery steam generator (HRSG) with three-stage pressure steam turbine (HPST, IPST and LPST).

First of all, the air is compressed by an air compressor and is mixed with natural gas in a combustion chamber to provide oxygen required for the natural gas combustion process. The inlet temperature of the gas turbine is maintained constant by adjusting the feed air quantity, and then the flue gas enters the gas turbine to drive the impeller to generate electricity. Finally, the exhaust gas emitted by the gas turbine is discharged into the atmosphere in the form of flue gas after passing through the heat recovery steam generator and treated by CCS device. The HRSG consists of three steam generation systems, namely high-pressure evaporation, medium pressure evaporation and low-pressure evaporation systems, and drives the steam turbine to generate electricity in the form of a steam Rankine cycle. As shown in Fig. 2, the EGR process is to recycle a certain proportion of flue gas from the outlet of heat recovery steam generator (HRSG) to the air compressor inlet for mixing with fresh air. The EGR process increases the CO_2 concentration of the flue gas of the system, and the EGR process can reduce the loss of

Table 1
The summary of literature review.

Source	Years	Authors	Study details		System configuration	CCR (%)	Q_{unit} (MJ/kg CO_2)	Performance
			Method	Platform				
[21]	2012	N. Sipöcz	Simulation	IPSEpro/CO_2SIM	440 MW NGCC + MEA + EGR	90%	3.25–3.97	Power plant efficiency is 49.48–50.67%
[22]	2016	M. Pan et al.	Simulation	Aspen Plus	420 MW NGCC + MEA + EGR	90%	3.96	Comprehensive efficiency increased by 22%
[23]	2013	C. Biliyok et al.	Simulation	Aspen HYSYS	440 MW NGCC + MEA + EGR	90%	–	System power generation increased by 10 MW
[24]	2013	P.A. Marchioro Ystad et al.	Simulation	UniSim	439 MW NGCC + MEA + ORC	90%	2.67–3.95	Power plant efficiency is 50.4–58.46%
[25]	2014	J.K. Pandit et al.	Simulation	Aspen Plus	400 MW NGCC + MEA/UNO MK 3 [a] + EGR	85%	–	Power plant efficiency is 44.6–55.5%
[6]	2014	K. Lindqvist et al.	Simulation	Aspen HYSYS	416 MW NGCC + MEA + EGR	90%	3.97–4.28	Power plant efficiency is 49.45–50.36%
[1]	2015	X. Luo et al.	Simulation	Aspen Plus	453 MW NGCC + MEA + EGR	90%	4.31–4.54	Power plant efficiency is 49.16–58.74%
[10]	2017	Y. Hu, H. Ahn	Simulation	UniSim	569 MW NGCC/EGR + MEA	90%	–	Power plant efficiency is 47.2–57.2%
[26]	2014	T. Lambert et al.	Simulation	Aspen Plus	421 MW NGCC + MEA + EGR	75%	3.99–5.82	Total energy loss decreased from 15.3% to 13.6%
[7]	2017	Y. Hu et al.	Simulation	UniSim	555 MW NGCC + MEA + EGR	90%	4.14–4.70	Power plant efficiency is 46.95–55.55%
[5]	2017	G.G.Esquivel-Patiño et al.	Simulation	Aspen Plus	453 MW NGCC + MEA + ORC	~90%	–	Power plant efficiency is 50.69–58.49%
[27]	2018	S.-Y. Oh et al.	Simulation	Aspen Plus	550 MW Coal-fired + MEA	90%	3.21–3.97	Power plant efficiency is 26.5–30.6%
[9]	2019	Gerardo Geovanni et al.	Simulation	Aspen Plus	453 MW NGCC + MEA + EGR + ORC	90%	–	Net power output is 381.2 MW- 391.41 MW
[28]	2016	Z. He et al.	Simulation	Aspen Plus	453 MW NGCC + MEA	90%	–	Dynamic system simulation provides operational strategies
[29]	2018	C. Nwaoha et al.	Simulation	ProMax	115 MW Coal-fired + MEA–DEA	90%	2.75–4.25	Reduce energy consumption by mixing MEA and DEA
[30]	2018	P.L. Mores et al.	Simulation	GAMS	420 MW NGCC + MEA	> 90%	–	The mitigation cost is 90.88 \$/t CO_2
[31]	2019	Pérez Sánchez et al.	Simulation	Aspen HYSYS	400 MW NGCC + MEA + EGR	90%	3.14–3.68	LOCE[b] is reduced by \$10
[32]	2019	A.MAlcaráz-Calderon et al.	Simulation	Aspen Plus	674 MW NGCC + EGR + MEA	90%	3.58–3.62	Power plant efficiency is 45.9–52.1%
[33]	2017	J. Wang et al.	Simulation	Aspen Plus	300 MW Coal-fired + MEA + solar	90%	3.54	Power plant efficiency is 26.55–33.65%
[34]	2019	J. Wang et al.	Simulation	Aspen Plus	MEA	90%	–	The second law efficiency is around 28%
[35]	2019	J. Wang et al.	Simulation	Aspen Plus	300 MW Coal-fired + MEA + solar	70–90%	3.34–3.54	Power plant efficiency is 29.04–38.54%
[36]	2019	Y. Xu et al.	Simulation	Aspen Plus	MEA	–	2.82–4.97	The evaluation parameter COP_{CO2} is put forward.

Note: UNO MK 3[a]: Absorption solvent; LOCE[b]: Levelized cost of electricity; DEA[c]: Diethanolamine.

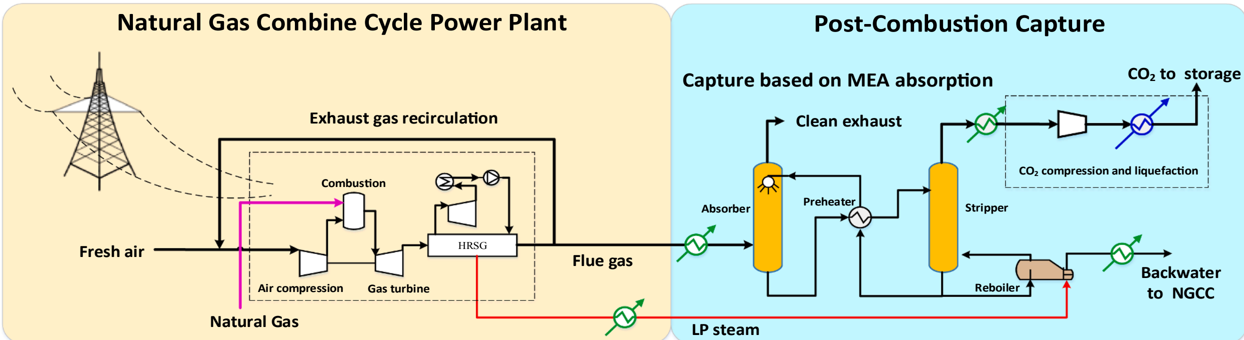

Fig. 1. Schematic diagram of NGCC power plant with PCC process.

the system without changing the configuration of the main body of the power plant. And it can reduce the mass flow into the PCC system and reduce the energy consumption and equipment size required for the capture process [1].

2.2. Description of PCC process

The PCC process is mainly composed of CO_2 capture process and CO_2 compression process, and the schematic diagram is given in Fig. 3. The flue gas from the outlet of HRSG flows into the absorption tower after being pretreated and is absorbed by the absorbent from the top of the tower. The capture process uses the MEA solution to absorb CO_2 from the flue gas, and the gas containing a small amount of CO_2 at the top of the column is discharged into the atmospheric environment. The liquid at the bottom of the absorption tower is preheated by the stream from the bottom of the stripping tower and then enters the stripping tower. The CO_2 is extracted from the top of the tower and the lean solvent at the bottom of the tower is cooled by internal heat exchange which returns to the absorption tower to complete the absorption process. In order to transport and store the captured CO_2 at room temperature, it is necessary to separate and purify the CO_2 from the stripping tower, and compress it above the supercritical pressure. The CO_2/H_2O mixture from the stripper column is dewatered by the separation device, and then the CO_2 is condensed to the saturated liquid phase through the ammonia refrigeration cycle. The liquid CO_2 is compressed to 150 bar [38,39] by the pump for further storage.

2.3. ORC system and its improvement

From the literature review, it can be seen that ORC system can effectively make use of the process waste heat of NGCC-PCC system and reduce the efficiency penalty of the system [40]. The schematic diagram of basic ORC and its T-s diagram are shown in Fig. 4. After being pressurized by the working fluid pump, the organic working fluid is heated to saturation or overheating in the evaporator. Then it enters the turbine and drives the impeller to drive the generator for generating electricity. The exhaust vapor is then condensed to saturated liquid phase and returns to the inlet of the pump to complete the cycle.

The basic ORC system above has only one endothermic process and one exothermic process, which can make good use of a single heat source and heat sink in a small temperature range. However, there is a lot of waste heat at different temperature levels in NGCC-PCC system. Aiming at this problem, the double-pressure ORC system, as shown in Fig. 5, will be used to recover the waste heat at different temperature levels. To further improve the thermal efficiency of ORC, the regenerator will be added to the system. According to the T-s diagram in Fig. 5, the heat absorption process of the double-pressure ORC is different from that of basic ORC. Double-pressure ORC is a cycle that heat transfer with multiple different heat sources under two different pressures. One endothermic process is carried out in subcritical and the other is in supercritical.

In addition, this paper also integrates that LNG cold energy into the system. However, the direct utilization of LNG cold energy will cause the heat transfer temperature difference of cold and hot streams too large, resulting in large irreversible loss. Therefore, in order to reduce the irreversibility caused by the large temperature difference process of LNG cold energy utilization, the two-stage condensation Rankine cycle [41,42], as shown in Fig. 6, is used for energy integration. For the two-stage condensation Rankine cycle, the organic working fluid is divided into two streams and expanded to different condensing pressures after passing through the evaporator. As shown in Fig. 6(b), they are condensed to a saturated liquid phase through condensers, respectively,

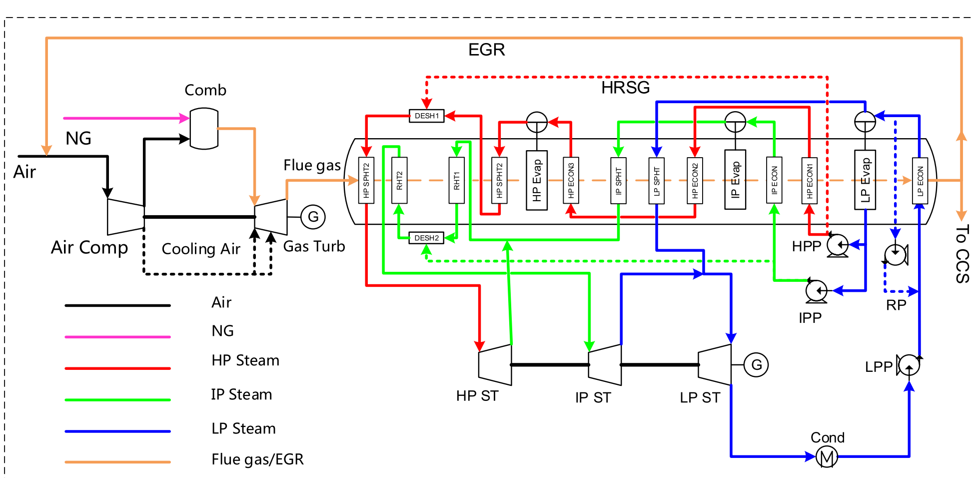

Fig. 2. Schematic diagram of the NGCC power plant process.

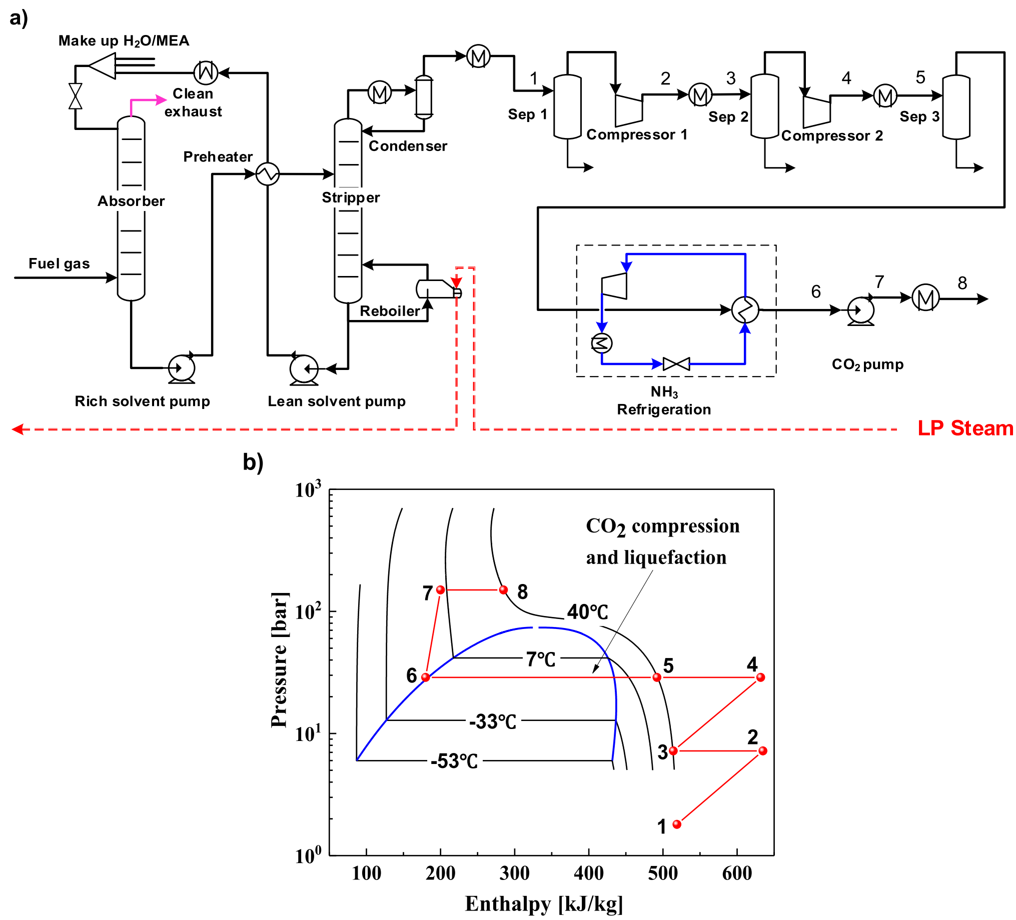

Fig. 3. a) Schematic diagram and b) P-H diagram of CO_2 compression and liquefaction process.

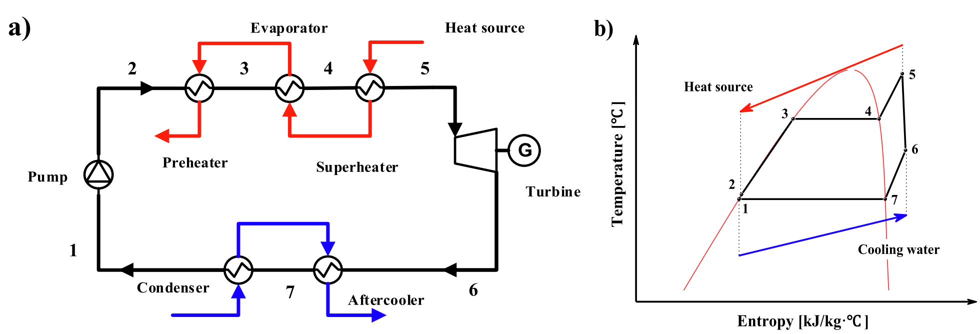

Fig. 4. a) Schematic diagram b) T-s diagram of the basic ORC process.

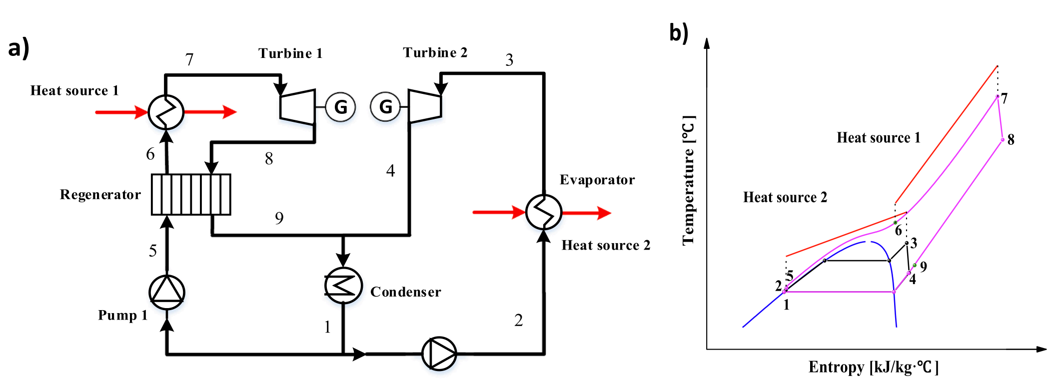

Fig. 5. a) Schematic diagram b) T-s diagram of the dual-pressure ORC process.

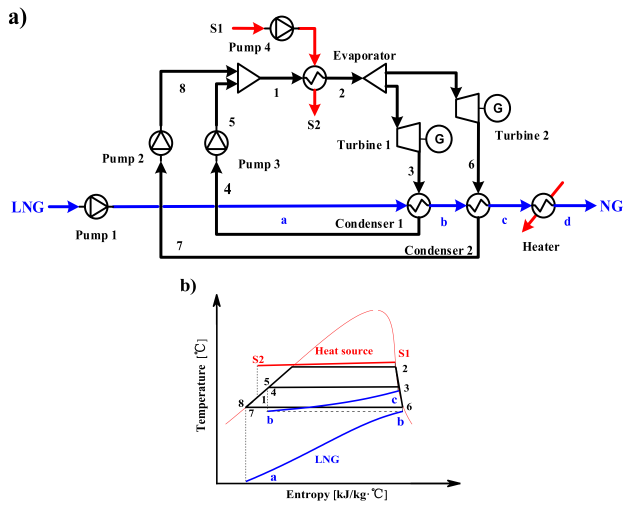

Fig. 6. a) Schematic diagram b) T-s diagram of the TSCRC progress.

and then mixed to flow into the evaporator by pump compression to complete the cycle.

3. Research methods

3.1. Model establishment

In order to analyze the system, the following assumptions are made in the simulation:

(1) LNG burns completely in the combustor and the NGCC power plant is at steady state.
(2) No leaks are occurred in the different configurations of the system [43].
(3) The gas and liquid in the absorption and desorption column are ideally distributed on each stage of the tray [44].
(4) The energy loss in the mixer and the separator, the friction loss with the pipe and the heat exchanger, and the heat loss are ignored.
(5) The heat exchange between the equipment and the environment in the system and the kinetic and potential energy during the cycle are negligible.

3.1.1. Energy analysis of NGCC power plant

For a NGCC power plant, the power output is composed of gas turbine and steam turbine, and the gas turbine and air compressor are connected by mechanical device. The net power output of the gas turbine is shown as follows [43]:

$$W_{GT} = (W_{gas\_turb} - W_{air\_comp}/\eta_{mech})\cdot\eta_{gen} \tag{1}$$

where the W_{gas_turb} is the gas turbine power output, W_{air_comp} is the air compression power consumption, η_{mech} is the mechanical efficiency, and η_{gen} is the generator efficiency.

The net power output of the steam turbine can be expressed as follows [43]:

$$W_{ST} = (W_{HPST} + W_{IPST} + W_{LPST})\cdot\eta_{gen} - (W_{HPP} + W_{IPP} + W_{LPP} + W_{RP}) \tag{2}$$

where the W_{IPST}, W_{IPST} and W_{LPST} are the mechanical work of high-pressure, medium-pressure and low-pressure steam turbines, respectively, and W_{HPP}, W_{IPP}, W_{LPP} and W_{RP} are the power consumption of high-pressure, medium-pressure, and low-pressure recirculation pump in power plant, respectively.

The total power output of NGCC power plant can be described as follows:

$$W_{net\_NGCC} = W_{GT} + W_{ST} \tag{3}$$

3.1.2. Energy analysis of PCC process

For the CO_2 capture progress, the main parameters are the CO_2 capture rate and the energy consumption required for the CO_2 per unit mass. The CO_2 capture rate CCR [44] is represented by the molar ratio of the captured CO_2 to the CO_2 entering the system.

$$CCR = \dot{n}_{CO_2\_captured}/\dot{n}_{CO_2\_in} \tag{4}$$

The formula for the energy consumption of unit mass CO_2 captured is as follows:

$$Q_{unit} = Q_{reboiler}/\dot{m}_{CO_2\_captured} \tag{5}$$

where $Q_{reboiler}$ is the energy consumption of reboiler, and $\dot{m}_{CO_2\_captured}$ is the mass flow rate of captured CO_2.

CO_2 compression energy consumption $W_{CO_2\_PC}$ is:

$$W_{CO_2\_PC} = \sum W_{comp} + W_{pump\_CO_2} \tag{6}$$

where there the $\sum W_{comp}$ including the power consumption of CO_2 compressors and refrigerant compression, $W_{pump\_CO_2}$ is the power consumption of CO_2 pump.

3.1.3. Energy analysis of double-pressure ORC and TSCRC

The net power output of the double-pressure ORC and TSCRC system can be described by the following formulas, respectively:

$$W_{net\_ORC-DP} = \sum W_{turb\_ORC-DP} - \sum W_{pump\_ORC-DP} \tag{7}$$

$$W_{net\_TSCRC} = \sum W_{turb\_TSCRC} - \sum W_{pump\_TSCRC} \tag{8}$$

3.1.4. Efficiency of power plants

The calorific value Q_{NG} of the combustion process of the power plant is provided by NG:

$$Q_{NG} = \dot{m}_{NG}\cdot LHV \tag{9}$$

where LHV is the low heating value of NG.

Auxiliary pump consumption W_{aux} consists of power consumption of cooling water and amine pump:

$$W_{aux} = \sum W_{water\_pumps} + \sum W_{NH_3\_pumps} \tag{10}$$

where $\sum W_{water\_pumps}$ is the total power consumption of the cooling water, and the $\sum W_{NH_3\_pumps}$ is the total power consumption of amine pump.

The total power output of NGCC power plant with different configurations are as follows:

$$W_{net\_TI} = \sum W_{NGCC+TI} - W_{CO_2\_PC} - W_{aux} \tag{11}$$

$$W_{net\_TI+ORC} = \sum W_{NGCC+TI} - W_{CO_2\_PC} - W_{aux} + W_{net\_ORC-DP} \tag{12}$$

$$W_{net\_TI+ORC+TSCRC} = \sum W_{NGCC+TI} - W_{CO_2\_PC} - W_{aux} + W_{net\_ORC-DP} + W_{net\_TSCRC} \tag{13}$$

where the W_{net_TI}, W_{net_TI+ORC} and $W_{net\_TI+ORC+TSCRC}$ represent the net power generation of the integrated scheme of NGCC + PCC + EGR + TI, NGCC + PCC + EGR + TI + ORC, and NGCC + PCC + EGR + TI + ORC + LNG, respectively.

The efficiency of basic NGCC power plant is:

$$\eta_{NGCC} = W_{net\_NGCC}/Q_{NG} \tag{14}$$

The NGCC power plant efficiency of each configuration is defined as the following:

$$\eta_{NGCC\_i} = W_{net\_i}/Q_{NG} \tag{15}$$

where i represents the different configured NGCC power plant.

The energy penalty of the different configured NGCC power plant [45] is as shown:

$$Energy\_penalty = 1 - \eta_{NGCC\_i}/\eta_{NGCC} \tag{16}$$

3.2. Model verification

The simulation of NGCC power plant with the PCC process is performed in the Aspen HYSYS 9.0 environment. Peng-Robinson equation is the state of equation for the gas turbine, dual-pressure ORC and TSCRC. ASME steam model [43] is used for the steam turbines, and Amine and the Kent-Eisenberg model for the CO_2 capture unit [46]. In order to verify the accuracy of the model, the NGCC power plant and CO_2 capture unit are verified, respectively.

3.2.1. Verification of the NGCC system

First of all, the gas turbine and steam turbine are simulated, and the NGCC power plant is consistent with that of Z. Liu and I.A. Karimi [43]. The design parameters including feed air, fuel gas composition and basic parameters, are given in Table 2 and Table 3, respectively.

The simulation results of NGCC power plant are shown in Table 4, and the results are in good agreement with the literature [43]. Therefore, the accuracy of the model is verified.

3.2.2. Verification of the PCC process

In this section, the CO_2 capture process based on MEA absorption is verified, and the operating parameters of the system are given in Table 5.

The main energy consumption of CO_2 capture process based on MEA is in the reboiler. Therefore, in order to verify the accuracy of the system, the energy consumption and capture rate of the system are compared with the work of S.-Y. Oh et al. [46]. The results are shown in Fig. 7, in which the solid line represents the simulation value and the dashed line represents the data of the reference. It can be seen from the figure that the CO_2 capture rate and the capture energy consumption of the unit CO_2 are almost consistent with the literature, which can prove the accuracy of the model.

4. Results and discussion

4.1. Basic case

The addition of carbon capture system will reduce the power generation efficiency of NGCC power plant. Firstly, the generation efficiency of NGCC power plant, the reduction of generation efficiency after adding PCC system and the influence of EGR process are determined. The typical capture rate of 90% [23,32,47] is selected for the study. In order to determine the EGR ratio, the variation of O_2 concentration, CO_2 concentration and the capture energy consumption of unit CO_2 with the EGR ratio are investigated, as shown in Fig. 8. With the increase of EGR ratio, the capture energy consumption Q_{unit} of unit CO_2 gradually decreases, while the CO_2 concentration in flue gas increases and the O_2 concentration decreases. When the oxygen concentration into the combustion chamber drops below 16%, the flame shape and flue gas temperature [22,47] in the combustion process will be affected. Therefore, the EGR ratio of 35% is selected in this paper. On this basis, NGCC, NGCC + PCC and NGCC + PCC + EGR systems are simulated, respectively, and the system parameters are shown in Table 6.

As can be seen from Table 5, a large amount of low-pressure steam is extracted due to the addition of the PCC process. Therefore, the power output of the low-pressure turbine is reduced, and the net power generation efficiency of the system is reduced from 55.88% to 48.09%. The amount of extracted steam is reduced from 67.33 kg/s to 62.90 kg/s on account of the EGR process, and the auxiliary energy consumption can also be reduced. The results show that the net power generation efficiency of the system is increased by 0.86%, and the energy penalty is reduced from 13.94% to 12.40% because of the addition of the EGR process. Therefore, the NGCC power plant with the PCC and EGR process is selected in the following research to further reduce the system energy penalty. For the purpose of comparison, NGCC + PCC + 35% EGR is defined as a basic case.

4.2. Case I. Integration of NGCC system with PCC and EGR process

During the simulation, it is found that there are a large number of hot and cold streams in the NGCC system with PCC and EGR processes. First, internal thermal integration is performed to recover system waste heat, reduce system utilities consumption and increase system power generation efficiency, due to its ease of modification.

The internal thermal integration is analyzed by pinch theory which is a thermal integration method based on thermodynamic process and principle proposed by Linnhoff and Hindmarsh (1983) [48,49]. The energy consumption of the system is reduced by strengthening the heat exchanger network of the whole system of the NGCC power plant, and the minimum amount of cold and hot utilities is obtained. The inlet and outlet temperature of the streams in the system and the corresponding heat capacity need to be provided in this process. Through the analysis of NGCC power plant, it is found that there are 8 hot streams and 2 cold streams in the system, as shown in Fig. 9.

The heat streams are as follows: H1-H7 are the waste heat of the LP steam, the second stage compressor, the first stage compressor, the reboiler backwater, the stripping tower top, flue gas and CO_2 condensation, respectively. H8 is a saturated steam that is formed by the superheated steam cooling process [10,14,15]. The cold streams are as follows:C1 is the natural gas at the entrance of the combustion chamber, and C2 is the stream at the bottom of the stripping tower. In the whole process, the pinch temperature is 10 °C [43,50] (except the refrigeration system). The inlet temperature, outlet temperature and heat capacity of the hot and cold streams are given in Table 7.

According to the data of the hot and cold streams in Table 6, the composite curves of the NGCC power plant with PCC and EGR process are obtained by question table method, as shown in Fig. 10. It can be seen from the figure that the maximum heat transfer inside the system is 141.84 MW. The net output power of the system is improved by heat match between the streams. The heat exchange network can be obtained as shown in Fig. 11 and the new system is defined as case 1 for simplicity.

As can be seen from Fig. 11, three heat exchangers need to be added during the thermal integration process, namely:

(1) Heat exchanger 1: the waste heat of the first-stage compressor H3 is used for preheating of the bottom stream of the stripper tower.
(2) Heat exchanger 2: the waste heat of the second-stage compressor H2 is used for preheating of the bottom stream of the stripper

Table 2
Parameters of NGCC power plant feed gas.

Parameters	Air	Fuel
flow (kg/s)	635.0	14.74
Temperature (°C)	15.0	10.0
Pressure (bar)	1.0	30.0
LHV (kJ/kg)	—	47493.0
N_2	77.3%	1.47%
O_2	20.74%	—
H_2O	1.01%	—
CO_2	0.03%	0.68%
Ar	0.92%	—
CH_4	—	87.08%
C_2H_6	—	7.83%
C_3H_8	—	2.94%

Table 3
Model parameters of NGCC process.

Component	Model	Value
Gas turbine (GT)	Compressor pressure ratio	15.4
	Compressor isentropic efficiency (%)	88.0
	Combustor exit temperature (°C)	1405.0
	Turbine inlet temperature (°C)	1328.0
	Turbine exhaust temperature (°C)	615.0
Heat Recovery steam generator (HRSG)	HP steam temperature (°C)	565.0
	IP steam temperature (°C)	297.0
	LP steam temperature (°C)	295.0
	HP/IP/LP pinch point temperatures (°C)	10.0
Steam turbines (STs)	HP/IP/LP inlet pressure (bar)	98.8/24.0/4.0
	HP/IP/LP ST isentropic efficiency (%)	87.0/91.0/89.0
Condenser	Pressure (bar)	0.074
	Cooling water inlet temperature (°C)	25.0
	Cooling water temperature rise (°C)	10.0
Generator	Generator efficiency (%)	98.5

Table 4
Comparison of NGCC simulation results with literature.

Performance	Literature [43]	Simulation
GT power (MW)	253.2	253.6
ST power (MW)	139.8	139.87
Plant net power (MW)	393.0	393.47
Plant efficiency (%)	56.14	56.21

Table 5
Model parameters of PCC process [46].

Parameter	Value	
Inlet gas composition (mol%)	N_2	76.65
	O_2	12.91
	H_2O	6.71
	CO_2	3.73
Inlet gas temperature/pressure (°C/bar)	40/1.1	
Lean solvent temperature/pressure (°C/bar)	40/1.1	
Inlet gas flow rate (kmol/h)	85,000	
Lean solvent flow rate (kmol/h)	120,000	
Number of stages/pressure in absorber (bar)	10/1.1	
Number of stages/pressure in stripper (bar)	6/2.0	

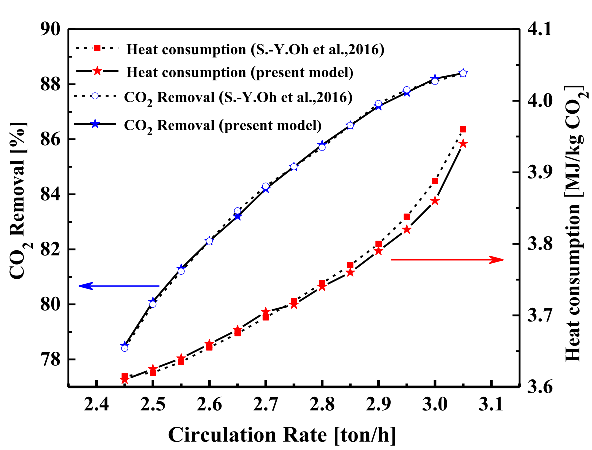

Fig. 7. Comparison of the results between simulation and literature for PCC process.

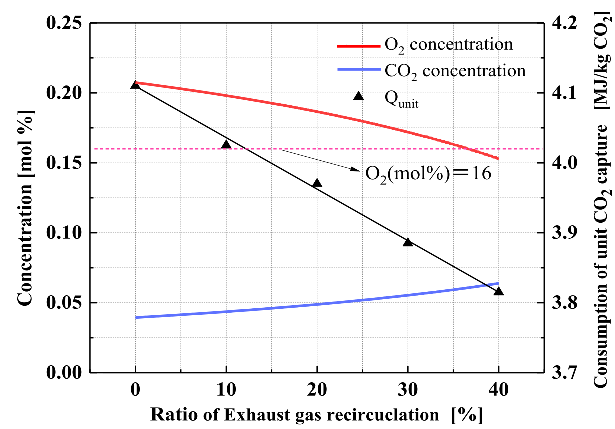

Fig. 8. The influence of EGR ratio on (a) O_2 concentration (b) CO_2 concentration (c) Energy consumption of unit CO_2.

Table 6
Performance of NGCC, NGCC + PCC and NGCC + PCC + EGR systems.

Case	NGCC	NGCC + PCC	NGCC + PCC + EGR
Gas turbine power	**257.51**	**257.51**	**253.9**
Gas turbine	507.09	507.09	529.8
Air compressor	249.58	249.58	275.9
Steam turbine power	**142.69**	**100.58**	**110.22**
HP turbine	28.49	28.49	29.47
IP turbine	47.94	47.94	50.25
LP turbine	66.26	24.19	30.50
Circulating Pumps	1.33	1.33	1.35
CW pump	1.53	0.56	0.70
Post Captured Aux		**1.14**	**1.10**
Steam extraction kg/s	—	67.33	62.90
Specific power consumption	—	4.11	3.85
Lean pump	—	0.239	0.218
Rich pump	—	0.117	0.109
CW pumps	—	0.784	0.780
CO_2 Compression		**13.12**	**13.12**
CO_2 compressor	—	12.96	12.96
CW pumps	—	0.163	0.163
Total power generation	**394.20**	**352.72**	**358.64**
Net power	**391.19**	**336.56**	**342.40**
Net power efficiency (%)	**55.88**	**48.08**	**48.91**
Energy penalty (%)	**—**	**13.95**	**12.46**

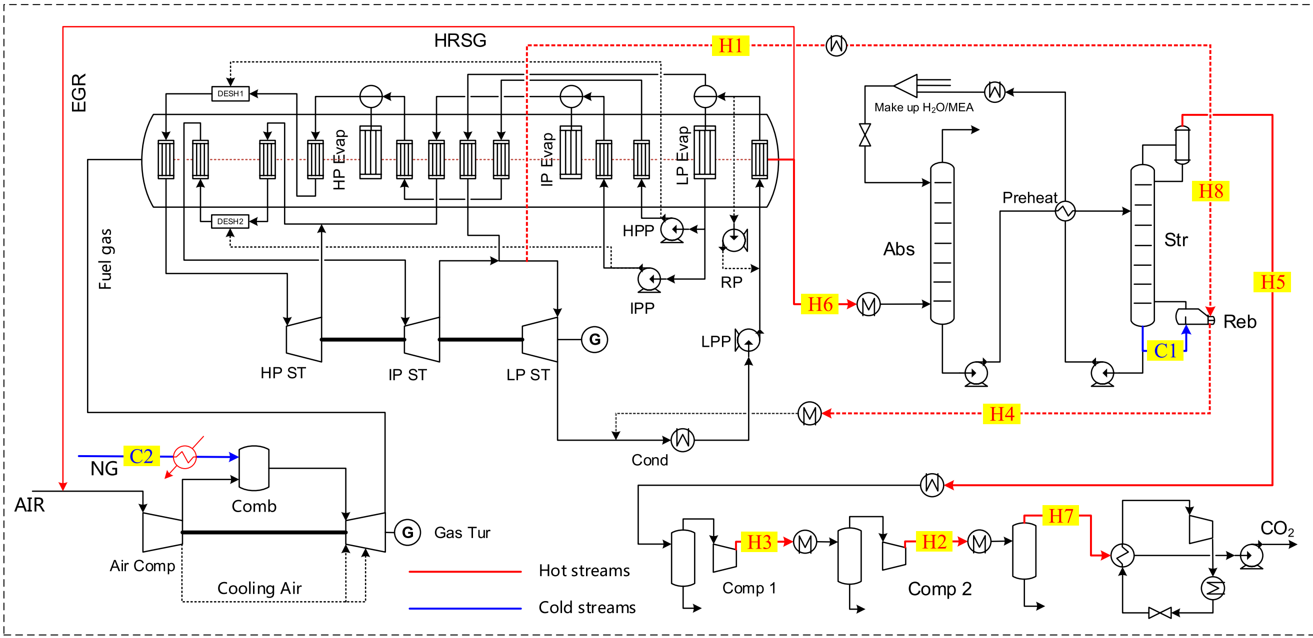

Fig. 9. Hot and cold streams of the NGCC system with PCC and EGR processes.

Table 7
Hot and cold streams of the NGCC power plant.

Streams	T_{in} (°C)	T_{out} (°C)	FCp (kW/K)	Duty (kW)
H1	295.0	140.0	131.87	20,440
H2	176.4	40.0	39.32	5292
H3	170.4	40.0	43.89	5245
H4	128.3	40.0	264.55	23,360
H5	101.9	40.0	559.77	34,650
H6	99.03	40.0	640.06	37,770
H7	40.0	−5.0	241.93	10,150
H8	140.0	128.3	11794.87	138,000
C1	10.0	120	34.93	3843
C2	118.3	120	81176.47	138,000

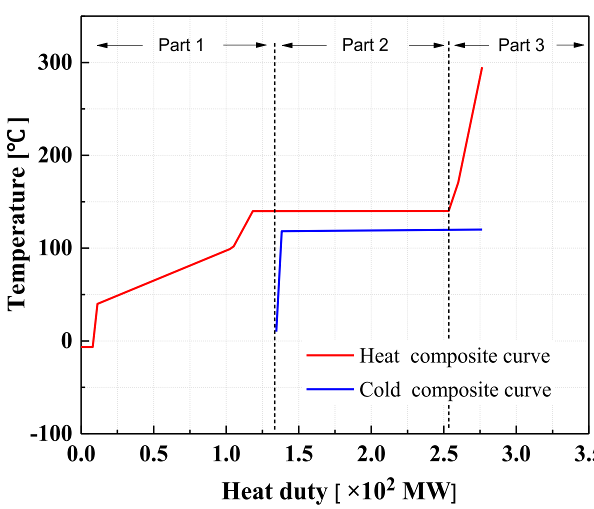

Fig. 10. Composite curves of the NGCC power plant with PCC and EGR process.

tower.

(3) Heat exchanger 3: the waste heat of the first-stage compressor H3 is used for preheating of natural gas.

Because the heat exchanger 1 and 2 preheat the bottom stream of the stripping tower, the amount of the extraction steam is reduced from 62.90 kg/s to 61.53 kg/s, and the energy consumption of CO_2 capture is reduced. Therefore, the net power generation of the NGCC power plant is improved. With the increase of natural gas inlet temperature, the net output power of the gas turbine and the steam turbine will be slightly increased under the condition that the key parameters of the system remain unchanged. The system flowsheet after thermal integration is shown in Fig. 12.

The system performance of the internal thermal integration process is shown in Table A1 of appendix. As can be seen from the Table, the net power output in the integrated system has been slightly improved. The net output work of case 1 NGCC + PCC + EGR + TI is 0.59% higher than that of basic case NGCC + PCC + EGR. The structure of internal thermal integration process is simple and easy to realize. The amount of cold utilities can be reduced by thermal integration process, but it can also be seen from the total composite curve that there is still a large amount of waste heat in the system that cannot be integrated into the system effectively.

4.3. Case II. NGCC + PCC + EGR + TI + ORC

It can be seen from section 4.2 that there is a lot of waste heat at different temperature levels in the case 1 system. According to the temperature of waste heat, the parameters such as the working fluid of ORC, the inlet and outlet temperature of streams, the evaporation pressure and condensation pressure are shown in Table 8. The parameters of streams after integrating the double-pressure ORC system are shown in Table 9.

Fig. 13 shows the composite curve of NGCC + PCC + EGR + TI + ORC system, known as case 2, which is the NGCC power plant incorporating ORC process. It can be seen that the maximum heat transfer capacity of the system increases, and the matching of streams at the high and low temperature level is improved, as shown in the first and third parts of the diagram. The analysis of the heat exchanger network is carried out after the parameters of the streams are obtained, and the result is shown in Fig. 14.

As seen from Fig. 14, four additional heat exchangers are required for the utilization of waste heat in double-pressure ORC, which are as follow:

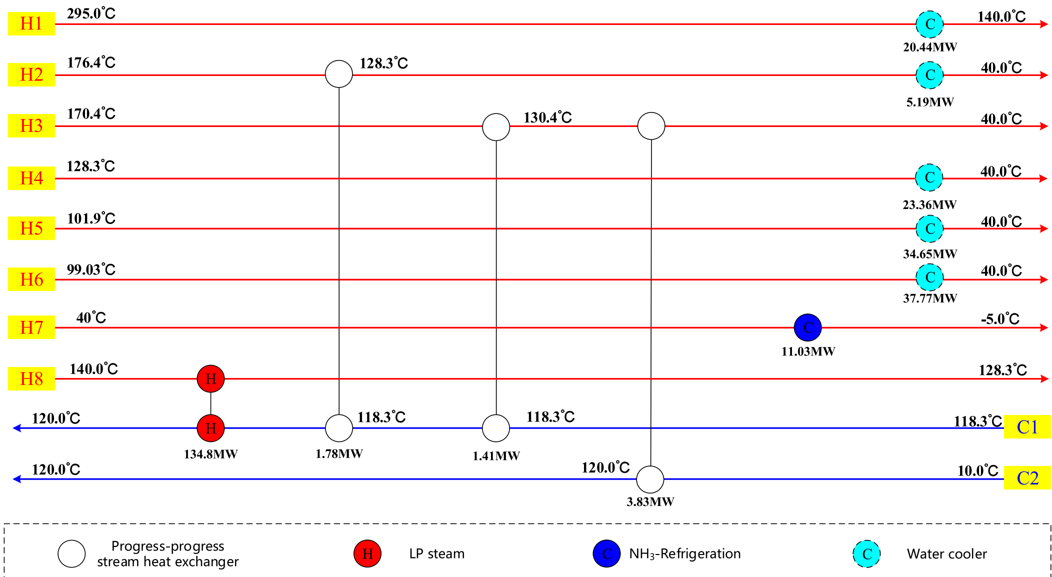

Fig. 11. The heat exchanger network of case 1.

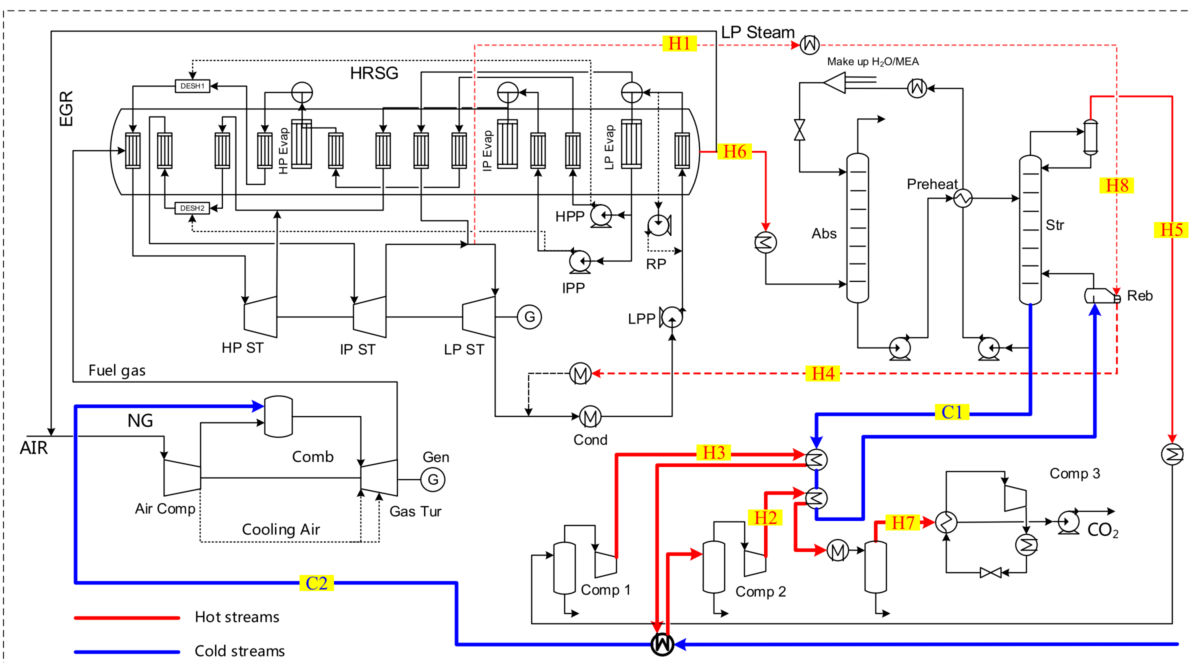

Fig. 12. Flowsheet of the NGCC power plant in case 1 NGCC + PCC + EGR + TI.

Table 8
Working fluid and system parameters of dual-pressure ORC.

Parameter	Value
Working fluid	R245fa
Pinch temperature (°C)	10.0
Turbine isentropic efficiency (%)	80
Pump isentropic efficiency (%)	75
Condensation temperature (°C)	40.0
Inlet temperature of LP-ORC (°C)	40.2
Inlet temperature of HP-ORC (°C)	130.0
Turbine inlet temperature/pressure of LP-ORC (°C/bar)	118.0/6
Turbine inlet temperature/pressure of HP-ORC (°C/bar)	260.0/30

(1) Heat exchanger 1: the waste heat of superheated steam H1 is used to heat the working fluid of high-pressure loop for dual-pressure ORC cycle.
(2) Heat exchanger 2: the waste heat of steam backwater H4 makes the working fluid of low-pressure loop for dual-pressure ORC cycle evaporate.
(3) Heat exchanger 3: the waste heat of stripping tower top H5 preheats the working fluid of low-pressure loop for dual-pressure ORC cycle.
(4) Heat exchanger 4: the working fluid of low-pressure loop for dual-pressure ORC cycle is preheated by the waste heat of flue gas H6.

Due to the addition of double-pressure ORC, the maximum heat transfer capacity of the system is increased. In this process, a large amount of heat source at different temperature in the system are utilized through the ORC process, and the net output power of the NGCC

Table 9
The streams for the NGCC power plant with dual-pressure ORC.

Streams		Type	T_{in} (°C)	T_{out} (°C)	FCp (kW/K)	Duty (kW)
System	H1	Hot	295.0	140.0	128.96	19,990
	H2	Hot	176.4	40.0	39.32	5195
	H3	Hot	170.4	40.0	43.89	5244
	H4	Hot	128.3	40.0	264.55	23,360
	H5	Hot	101.9	40.0	559.77	34,650
	H6	Hot	99.0	40.0	640.06	37,770
	H7	Hot	40.0	−5.0	241.93	10,150
	H8	Hot	140.0	128.3	11521.36	134,800
	C1	Cold	118.3	120.0	81176.47	138,000
	C2	Cold	10.0	120.0	34.93	3843
ORC	ORC-H1	Hot	82.32	40.0	242.69	63,109
	ORC-C1	Cold	40.2	118.0	278.35	50,815
	ORC-C2	Cold	130.0	260.0	153.77	19,990

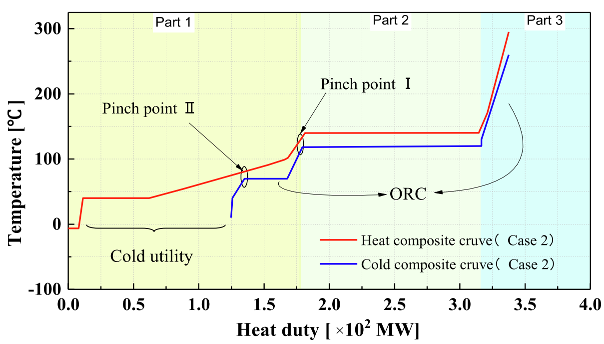

Fig. 13. Composite curves of NGCC power plant incorporating ORC streams for case 2.

power plant system is significantly improved. The result of case 2 NGCC + PCC + EGR + TI + ORC is given in Table A1 of appendix. According to Table A1 of appendix, the power generation of case 2 system is 354.64 MW. Compared with case 1, the power generation and power generation efficiency are increased by 7.721 MW and 1.12%, respectively, and the energy penalty is reduced from 11.3% to 9.3%.

Table 10
Working fluid and system parameters of TSCRC.

Parameter	Value
Working fluid	CH_3F
Pinch temperature (°C)	5
Turbine isentropic efficiency (%)	80
Pump isentropic efficiency (%)	75
First condensation temperature (°C)	−80.4
Second condensation temperature (°C)	−46.0
Evaporation temperature (°C)	15.0

4.4. *Case III. NGCC + PCC + EGR + TI + ORC + LNG*

Through the analysis of section 4.3, it can be found that there is still a large amount of waste heat energy in case 2 system, but the temperature is low (about 90 °C). At this time, a large amount of cold utilities is required in the power plant to cool the low-temperature heat streams. For the NGCC power plant, NG comes from LNG tanks with a large amount of cold energy. Low temperature LNG is usually heated by seawater, which means that the cold energy of LNG is released into the environment through seawater, resulting in a waste of cold energy. The irreversible loss of the system is large because the temperature difference of heat transfer is large when the cold energy at −162 °C is used directly. The LNG cold energy can be used for power generation by two-stage condensation Rankine cycle, which avoids the large irreversible loss caused by direct utilization of LNG cold energy. In this section, in order to further improve the integration system performance, the LNG cold energy is integrated into NGCC power plant through two-stage condensation Rankine cycle (TSCRC). The parameters of TSCRC system are given in Table 10. New hot and cold streams are formed in the system, in which C2 takes into account the utilization process of cold energy in the low temperature section of LNG. As a result, the inlet temperature of LNG cold stream C2 has changed from 10 °C to −162 °C.

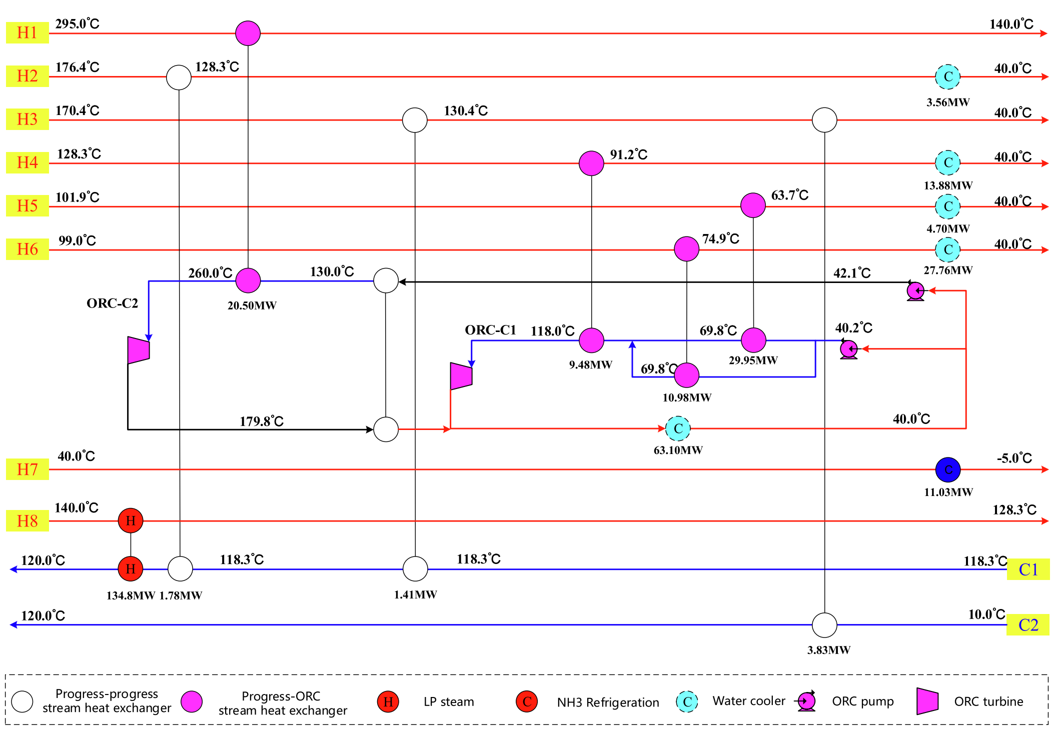

Fig. 14. Heat exchanger network diagram of case 2 (NGCC + PCC + EGR + TI + ORC).

Table 11
New stream data after considering LNG cold energy in case 3.

Streams	Type	T_{in} (°C)	T_{out} (°C)	FCp (kW/K)	Duty (kW)
C2	Cold	−162.0	120.0	35.79	6120
TSCRC-C1	Cold	−67.4	15.0	49.87	11,230
TSCRC-H1	Hot	−46.0	−46.0	–	3176
TSCRC-H2	Hot	−80.4	−80.4	–	6218

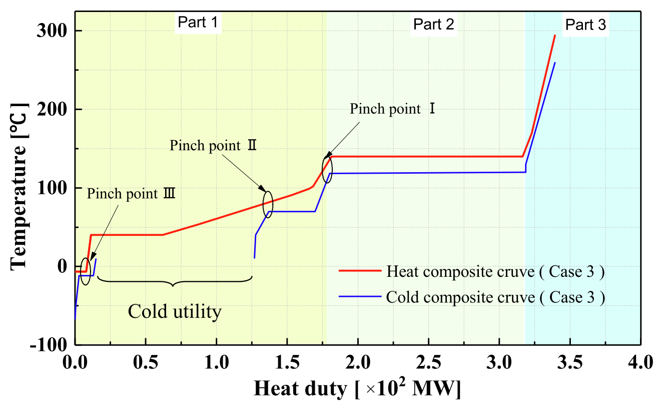

Fig. 15. Composite curves of NGCC power plant incorporating LNG streams case 3 NGCC + PCC + EGR + TI + ORC + LNG.

Table 11 shows the stream data, which is added after considering the TSCRC system, and the other streams are the same as the case 2.

According to the data of hot and cold streams, the composite curves of case 3 are given in Fig. 15. It can be found that the maximum heat transfer capacity of the system is further increased, and the amount of cold utilities in the system is reduced due to the addition of LNG cold energy. In order to make full use of the cold energy, the analysis of the heat transfer network of the system is carried out and the diagram of the heat exchange network is as shown in Fig. 16.

As seen from Fig. 16, five heat exchangers need to be added to the NGCC power plant with integrated utilization of LNG cold energy as follows:

(1) Heat exchangers 1 and 2: the LNG cold energy C2 is used for liquefaction of different pressure working fluid in TSCRC process.
(2) Heat exchanger 3: LNG cold energy C2 is used for inter-cooling of compressor stage 2.
(3) Heat exchanger 4 and 5: working fluid C1 of TSCRC is used in CO_2 liquefaction and dual-pressure ORC condensation process, respectively.

For heat exchanger 1 and 2, LNG cold energy is used as the heat sink of TSCRC to condense its working fluid, which reduce the irreversible loss of utilization of LNG cold energy. The use of the remaining part of LNG cold energy reduces the system's cold utilities in the heat exchanger 3. In heat exchanger 4, the evaporation process of TSCRC process is used in CO_2 liquefaction process, and the amount of system's cold utilities is further reduced in heat exchanger 5. In addition, the external refrigeration system in case 2 is replaced by the heat exchanger 4.

The two-stage condensation Rankine cycle is used as a medium for the integration process of case 3, which enables LNG cold energy to be closely integrated with the NGCC power plant. The performance of the

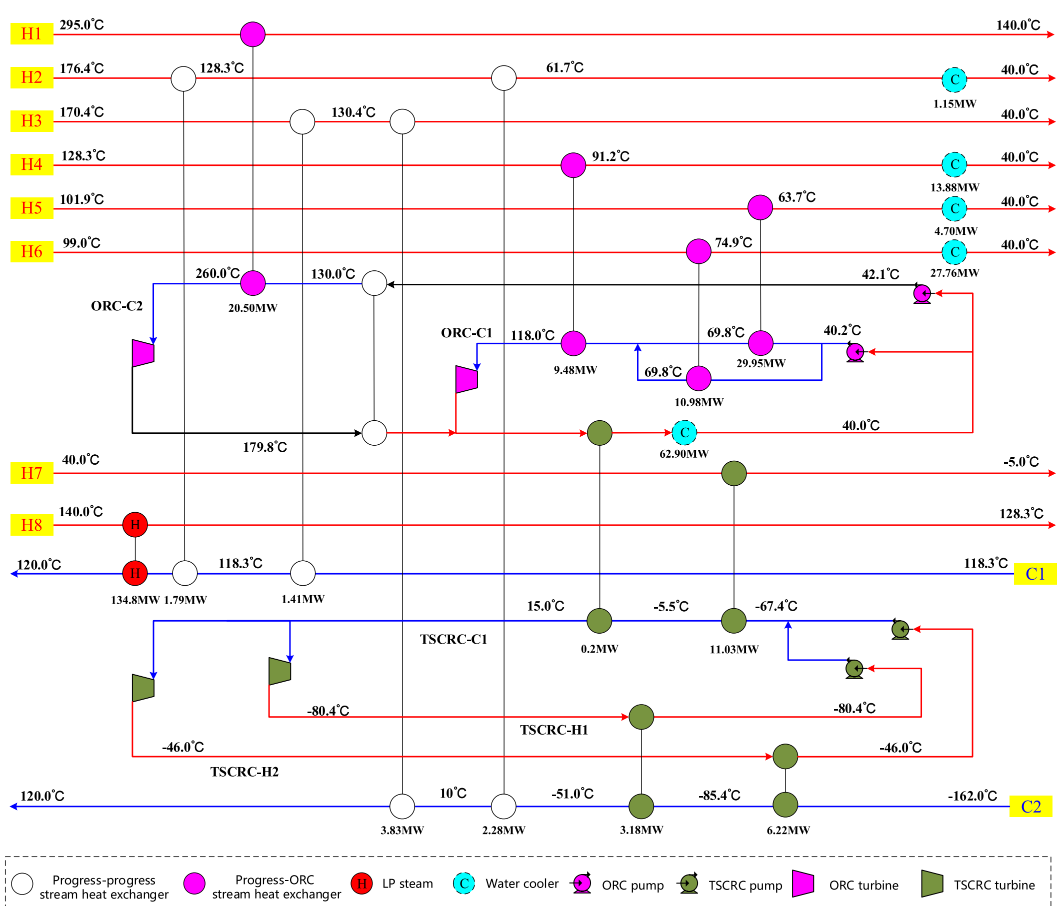

Fig. 16. Heat exchanger network diagram of case 3.

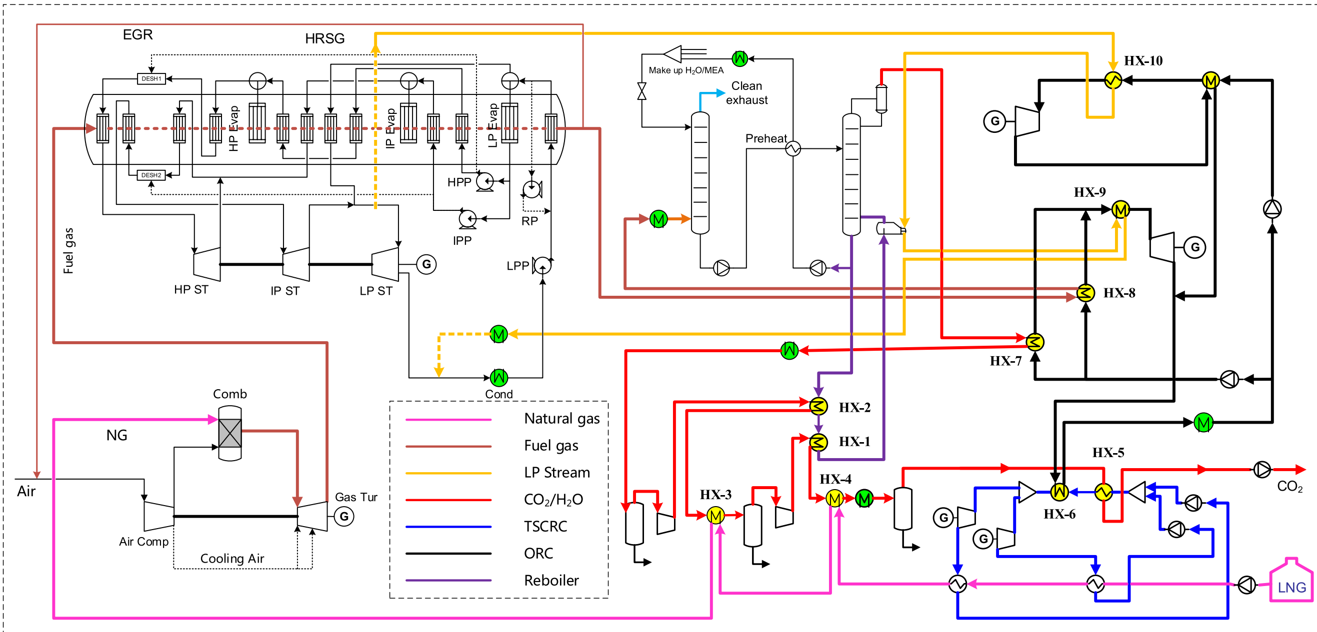

Fig. 17. Flowsheet of the NGCC power plant in case 3 NGCC + PCC + EGR + TI + ORC + LNG.

system is improved and the performance parameters are given in the appendix Table A1. For case 3, the LNG cold energy is firstly used to generate electricity by the two-stage condensation Rankine cycle, and the net power generation is 1.761 MW. The temperature of LNG in the system is increased, and then it is used in the CO_2 condensation process. And the power consumption of CO_2 capture system is reduced in the process of integration, which makes full use of the cold energy of LNG and reduces the use of utilities. Then the energy integration process of case 3 is summarized and the detailed data are given in Table A1 of appendix. It can be found that the net output power of the case 3 reaches 360.22 MW, and the power generation efficiency is increased to 51.46%, and the energy penalty of the power plant is reduced to 7.9%. Finally, the flowsheet of case 3 is given in Fig. 17.

5. Conclusion

The high energy consumption demand of the PCC process for the NGCC power plant will lead to a significant reduction in power generation efficiency. However, a large amount of low-temperature waste heat in NGCC power plant is difficult to be used due to its low temperature level. In this paper, the idea of integrating LNG cold energy with the NGCC power plant with PCC process is proposed. For the NGCC power plant of 391 MW with the PCC process, the model of the NGCC power plant is established and verified. The integration of the system is carried on to reduce the energy penalty. The following conclusions are obtained:

(1) When the NGCC power plant is combined with the PCC device based on MEA absorption process, the power generation efficiency of the power plant is reduced from 55.88% to 48.09%, which is mainly due to the high energy consumption of the compression process and the extraction of the low-pressure steam. Under the condition of 35% EGR cycle ratio, the power generation efficiency of the system is increased from 48.09% to 48.95% because the EGR process can increase the CO_2 concentration at the inlet of the PCC progress. Through internal thermal integration, the efficiency is increased by 0.59% by increasing the inlet temperature of NG and reducing the amount of steam needed in the reboiler.
(2) The energy integration of ORC progress and the NGCC power plant is considered, because there are still a lot of waste heat at different temperature levels in the power plant. With the construction of double-pressure ORC, the internal waste heat of the system is utilized effectively. The power recovery of ORC system is 7.721 MW and the power generation efficiency of the system is increased from 49.54% to 50.66%.
(3) Since a large amount of low temperature waste heat cannot be utilized by double-pressure ORC, then the LNG cold energy is further integrated with the NGCC power plant. Firstly, the LNG cold energy is used to generate electricity, and the power generation is 1.761 MW. After that, the temperature of LNG in the system is increased, and then it is used in the CO_2 liquefaction process. Therefore, the CO_2 liquefaction device is also saved for the NGCC power plant. Compared with the basic case, the power output of the case 3 is increased by 17.55 MW, the total efficiency of power plant is increased by 2.51%, and the energy penalty is reduced to 7.9%.

Declaration of Competing Interest

None.

Acknowledgement

This research was financially supported by the National Natural Science Foundation of China (No. 51606025), MOST innovation team in key area (No. 2016RA4053) and the Fundamental Research Funds for the Central Universities (Grant No. DUT19JC05).

Appendix

Table A1
Performance of various integrated NGCC power plants.

Case	Case 1	Case 2	Case 3
Gas turbine power	**257.04**	**257.04**	**257.04**
Gas turbine	532.89	532.89	532.89
Air compression	275.86	275.86	275.86
Steam turbines power	**111.29**	**111.29**	**111.29**
HP turbine	29.51	29.51	29.51
IP turbine	50.32	50.32	50.32
LP turbine	31.46	31.46	31.46
circulating water pumps	1.35	1.35	1.35
HPP	1.241	1.241	1.241
IPP	0.072	0.072	0.072
LPP	0.143	0.143	0.143
RP	0.021	0.021	0.021
CW pumps	0.680	0.680	0.680
Post Captured Aux	**1.107**	**1.107**	**1.107**
Steam extraction kg/s	61.44	61.44	61.44
Specific power consumption	3.83	3.83	3.83
Lean pump	0.218	0.218	0.218
Rich pump	0.109	0.109	0.109
Auxiliary in capture unit	0.780	0.780	0.780
CO_2 Compression	**13.12**	**13.12**	**9.32**
CO_2 compressor	12.96	12.96	9.242
CW pump	0.163	0.163	0.078
ORC		**7.721**	**7.721**
Turbines		8.176	8.176
Pumps		0.457	0.455
TSCRC			**1.761**
Turbines			1.803
Pumps			0.042
Total power generation	**362.81**	**370.41**	**372.14**
Net power	**346.44**	**354.02**	**359.56**
Net power efficiency (%)	**49.49%**	**50.57%**	**51.36%**
Energy penalty (%)	**11.4%**	**9.4%**	**8.0%**

References

[1] Luo X, Wang M, Chen J. Heat integration of natural gas combined cycle power plant integrated with post-combustion CO_2 capture and compression. Fuel 2015;151:110–7.

[2] Freeman J, Hellgardt K, Markides CN. An assessment of solar-powered organic Rankine cycle systems for combined heating and power in UK domestic applications. Appl Energy 2015;138:605–20.

[3] Chaychizadeh F, Dehghandorost H, Aliabadi A, Taklifi A. Stochastic dynamic simulation of a novel hybrid thermal-compressed carbon dioxide energy storage system (T-CCES) integrated with a wind farm. Energy Convers Manage 2018;166:500–11.

[4] Liu Q, Shen A, Duan Y. Parametric optimization and performance analyses of geothermal organic Rankine cycles using R600a/R601a mixtures as working fluids. Appl Energy 2015;148:410–20.

[5] Esquivel-Patiño GG, Serna-González M, Nápoles-Rivera F. Thermal integration of natural gas combined cycle power plants with CO_2 capture systems and organic Rankine cycles. Energy Convers Manage 2017;151:334–42.

[6] Lindqvist K, Jordal K, Haugen G, Hoff KA, Anantharaman R. Integration aspects of reactive absorption for post-combustion CO_2 capture from NGCC (natural gas combined cycle) power plants. Energy. 2014;78:758–67.

[7] Hu Y, Xu G, Xu C, Yang Y. Thermodynamic analysis and techno-economic evaluation of an integrated natural gas combined cycle (NGCC) power plant with post-combustion CO_2 capture. Appl Therm Eng 2017;111:308–16.

[8] Jansen D, Gazzani M, Manzolini G, Dijk Ev, Carbo M. Pre-combustion CO_2 capture. Int J Greenhouse Gas Control 2015;40:167–87.

[9] Esquivel Patiño GG, Nápoles Rivera F. Global warming potential and net power output analysis of natural gas combined cycle power plants coupled with CO_2 capture systems and organic Rankine cycles. J Cleaner Prod 2019;208:11–8.

[10] Hu Y, Ahn H. Process integration of a Calcium-looping process with a natural gas combined cycle power plant for CO_2 capture and its improvement by exhaust gas recirculation. Appl Energy 2017;187:480–8.

[11] Zanganeh KE, Shafeen A. A novel process integration, optimization and design approach for large-scale implementation of oxy-fired coal power plants with CO2 capture. Int J Greenhouse Gas Control 2007;1:47–54.

[12] Jin B, Zhao H, Zheng C. Dynamic simulation for mode switching strategy in a conceptual 600 MWe oxy-combustion pulverized-coal-fired boiler. Fuel 2014;137:135–44.

[13] Hetland J, Kvamsdal HM, Haugen G, Major F, Kårstad V, Tjellander G. Integrating a full carbon capture scheme onto a 450MWe NGCC electric power generation hub for offshore operations: Presenting the Sevan GTW concept. Appl Energy 2009;86:2298–307.

[14] Berstad D, Anantharaman R, Blom R, Jordal K, Arstad B. NGCC post-combustion CO_2 capture with Ca/carbonate looping: efficiency dependency on sorbent properties, capture unit performance and process configuration. Int J Greenhouse Gas Control 2014;24:43–53.

[15] Seif El Nasr A, Nelson T, Kataria A, Abu-Zahra MRM. Benchmarking of a novel solid sorbent CO_2 capture process for NGCC power generation. Int J Greenhouse Gas Control 2015;42:583–92.

[16] Jiang L, Gonzalez-Diaz A, Ling-Chin J, Roskilly AP, Smallbone AJ. Post-combustion CO_2 capture from a natural gas combined cycle power plant using activated carbon adsorption. Appl Energy 2019;245:1–15.

[17] Merkel TC, Wei X, He Z, White LS, Wijmans JG, Baker RW. Selective exhaust gas recycle with membranes for CO_2 capture from natural gas combined cycle power plants. Ind Eng Chem Res 2012;52:1150–9.

[18] Scholes CA, Ho MT, Wiley DE, Stevens GW, Kentish SE. Cost competitive membrane—cryogenic post-combustion carbon capture. Int J Greenhouse Gas Control 2013;17:341–8.

[19] van der Spek M, Ramirez A, Faaij A. Challenges and uncertainties of ex ante techno-economic analysis of low TRL CO_2 capture technology: lessons from a case study of an NGCC with exhaust gas recycle and electric swing adsorption. Appl Energy 2017;208:920–34.

[20] Lillia S, Bonalumi D, Grande C, Manzolini G. A comprehensive modeling of the hybrid temperature electric swing adsorption process for CO_2 capture. Int J Greenhouse Gas Control 2018;74:155–73.

[21] Sipöcz N, Tobiesen FA. Natural gas combined cycle power plants with CO_2 capture – opportunities to reduce cost. Int J Greenhouse Gas Control 2012;7:98–106.
[22] Pan M, Aziz F, Li B, Perry S, Zhang N, Bulatov I, et al. Application of optimal design methodologies in retrofitting natural gas combined cycle power plants with CO_2 capture. Appl Energy 2016;161:695–706.
[23] Biliyok C, Yeung H. Evaluation of natural gas combined cycle power plant for post-combustion CO_2 capture integration. Int J Greenhouse Gas Control 2013;19:396–405.
[24] Marchioro Ystad PA, Lakew AA, Bolland O. Integration of low-temperature transcritical CO_2 Rankine cycle in natural gas-fired combined cycle (NGCC) with post-combustion CO2 capture. Int J Greenhouse Gas Control 2013;12:213–9.
[25] Pandit JK, Harkin T, Anderson C, Ho M, Wiley D, Hooper B. CO_2 emission reduction from natural gas power stations using a precipitating solvent absorption process. Int J Greenhouse Gas Control 2014;28:234–47.
[26] Lambert T, Hoadley A, Hooper B. Process integration of solar thermal energy with natural gas combined cycle carbon capture. Energy 2014;74:248–53.
[27] Oh S-Y, Yun S, Kim J-K. Process integration and design for maximizing energy efficiency of a coal-fired power plant integrated with amine-based CO_2 capture process. Appl Energy 2018;216:311–22.
[28] He Z, Ricardez-Sandoval LA. Dynamic modelling of a commercial-scale CO_2 capture plant integrated with a natural gas combined cycle (NGCC) power plant. Int J Greenhouse Gas Control 2016;55:23–35.
[29] Nwaoha C, Smith DW, Idem R, Tontiwachwuthikul P. Process simulation and parametric sensitivity study of CO_2 capture from 115 MW coal–fired power plant using MEA–DEA blend. Int J Greenhouse Gas Control 2018;76:1–11.
[30] Mores PL, Manassaldi JI, Scenna NJ, Caballero JA, Mussati MC, Mussati SF. Optimization of the design, operating conditions, and coupling configuration of combined cycle power plants and CO_2 capture processes by minimizing the mitigation cost. Chem Eng J 2018;331:870–94.
[31] Pérez Sánchez J, Aguillón Martínez JE, Mazur Czerwiec Z, Zavala Guzmán AM. Theoretical assessment of integration of CCS in the Mexican electrical sector. Energy 2019;167:828–40.
[32] Alcaráz-Calderon AM, González-Díaz MO, Mendez Á, González-Santaló JM, González-Díaz A. Natural gas combined cycle with exhaust gas recirculation and CO_2 capture at part-load operation. J Energy Inst 2019;92:370–81.
[33] Wang J, Zhao J, Wang Y, Deng S, Sun T, Li K. Application potential of solar-assisted post-combustion carbon capture and storage (CCS) in China: a life cycle approach. J Cleaner Prod 2017;154:541–52.
[34] Wang J, Sun T, Zhao J, Deng S, Li K, Xu Y, et al. Thermodynamic considerations on MEA absorption: Whether thermodynamic cycle could be used as a tool for energy efficiency analysis. Energy 2019;168:380–92.
[35] Wang J, Zhao J, Deng S, Sun T, Du Y, Li K, et al. Integrated assessment for solar-assisted carbon capture and storage power plant by adopting resilience thinking on energy system. J Cleaner Prod 2019;208:1009–21.
[36] Xu Y, Deng S, Zhao L, Yuan X, Fu J, Li S, et al. Application of the thermodynamic cycle to assess the energy efficiency of amine-based absorption of carbon capture. Energies 2019;12:2504.
[37] Goto K, Yogo K, Higashii T. A review of efficiency penalty in a coal-fired power plant with post-combustion CO_2 capture. Appl Energy 2013;111:710–20.
[38] Alabdulkarem A, Hwang Y, Radermacher R. Development of CO2 liquefaction cycles for CO_2 sequestration. Appl Therm Eng 2012;33–34:144–56.
[39] Xu G, Li L, Yang Y, Tian L, Liu T, Zhang K. A novel CO_2 cryogenic liquefaction and separation system. Energy 2012;42:522–9.
[40] Tian R, An Q, Zhai H, Shi L. Performance analyses of transcritical organic Rankine cycles with large variations of the thermophysical properties in the pseudocritical region. Appl Therm Eng 2016;101:183–90.
[41] Bao J, Lin Y, Zhang R, Zhang N, He G. Strengthening power generation efficiency utilizing liquefied natural gas cold energy by a novel two-stage condensation Rankine cycle (TCRC) system. Energy Convers Manage 2017;143:312–25.
[42] Bao J, Yuan T, Zhang L, Zhang N, Zhang X, He G. Comparative study of liquefied natural gas (LNG) cold energy power generation systems in series and parallel. Energy Convers Manage 2019;184:107–26.
[43] Liu Z, Karimi IA. Simulating combined cycle gas turbine power plants in Aspen HYSYS. Energy Convers Manage 2018;171:1213–25.
[44] Tock L, Maréchal F. Environomic optimal design of power plants with CO_2 capture. Int J Greenhouse Gas Control 2015;39:245–55.
[45] van den Broek M, Hoefnagels R, Rubin E, Turkenburg W, Faaij A. Effects of technological learning on future cost and performance of power plants with CO_2 capture. Prog Energy Combust Sci 2009;35:457–80.
[46] Oh S-Y, Binns M, Cho H, Kim J-K. Energy minimization of MEA-based CO_2 capture process. Appl Energy 2016;169:353–62.
[47] Herraiz L, Fernández ES, Palfi E, Lucquiaud M. Selective exhaust gas recirculation in combined cycle gas turbine power plants with post-combustion CO_2 capture. Int J Greenhouse Gas Control 2018;71:303–21.
[48] Yee TF, Grossmann. Simultaneous optimization models for heat integration-II. Heat exchanger network synthesis. Comput Chem Eng 1990;14:1165–85.
[49] Papoulias Soterios A, Grossmann Ignacio E. A structural optimization approach inprocess synthesis—II. Heat recovery networks. Computers Chem. Eng. 1983;7:707–21.
[50] Liu Z, Karimi IA. New operating strategy for a combined cycle gas turbine power plant. Energy Convers Manage 2018;171:1675–84.